

SCIENTIFIC REPORTS



OPEN

Functional Characterization of Two Elongases of Very Long-Chain Fatty Acid from *Tenebrio molitor* L. (Coleoptera: Tenebrionidae)

Tianxiang Zheng¹, Hongshuang Li¹, Na Han², Shengyin Wang², Jennifer Hackney Price³, Minzi Wang⁴ & Dayu Zhang^{1,2}

The elongases of very long chain fatty acid (ELOVL or ELO) are essential in the biosynthesis of fatty acids longer than C14. Here, two ELO full-length cDNAs (*TmELO1*, *TmELO2*) from the yellow mealworm (*Tenebrio molitor* L.) were isolated and the functions were characterized. The open reading frame (ORF) lengths of *TmELO1* and *TmELO2* were 1005 bp and 972 bp, respectively and the corresponding peptide sequences each contained several conserved motifs including the histidine-box motif HXXHH. Phylogenetic analysis demonstrated high similarity with the ELO of *Tribolium castaneum* and *Drosophila melanogaster*. Both *TmELO* genes were expressed at various levels in eggs, 1st and 2nd instar larvae, mature larvae, pupae, male and female adults. Injection of *dsTmELO1* but not *dsTmELO2* RNA into mature larvae significantly increased mortality although RNAi did not produce any obvious changes in the fatty acid composition in the survivors. Heterologous expression of *TmELO* genes in yeast revealed that *TmELO1* and *TmELO2* function to synthesize long chain and very long chain fatty acids.

Fatty acids (FAs) are molecules with a variety of biological functions including acting as energy sources and serving as components of cellular lipids and other molecules including eicosanoid hormones such as prostaglandins and leukotrienes¹. FAs are precursors of sphingolipids, glycerolipids², hydrocarbons^{3,4}, fatty alcohols and wax esters⁵, which can participate in many cell biological processes such as reproduction, growth, migration, differentiation, and apoptosis and are components of pheromones in various arthropod species^{6–8}.

Structurally, FAs are composed of long hydrocarbon chains that end in a carboxyl group and are classified based on the chain length and the number of double bonds. Fatty acids are roughly classified by length into the following groups: (1) Short Chain Fatty Acids (SCFA) which have five or fewer carbons, (2) Medium Chain Fatty Acids (MCFAs) which contain 6–12 carbons, (3) Long-Chain Fatty Acids (LCFAs), which contain more than 12 carbon atoms, and (4) Very Long-Chain Fatty Acids (VLCFAs), which contain 22 or more carbon atoms. Each class is associated with unique functions. For example, in mammals LCFAs act as ligands for peroxisome proliferator-activated receptors (PPARs) and regulate energy metabolism⁹ while VLCFAs have important anti-inflammatory roles¹⁰.

Fatty acid synthesis consists of a four-step cycle that includes condensation, reduction, dehydration and reduction steps and occurs primarily in the endoplasmic reticulum (ER)¹¹. Each cycle extends an initial acetyl-CoA by two carbons and can be repeated up to seven times to form palmitic acid (C16:0)². Further growth requires elongases of long or very long chain fatty acids (ELOVL or ELO) which can elongate C ≥ 14 fatty acids through a fatty acid condensation reaction. Elongases of very long chain fatty acids have been isolated from various organisms, including yeast, mammals, plants and other species^{12–14}.

While ELOVLs have been relatively well characterized in vertebrates, little is known about these enzymes in insects, even though LCFAs and VLCFAs are widespread among insect taxa^{15–20}. Although some ELOVLs were

¹School of Forestry and Biotechnology, Zhejiang A&F University, Linan, Zhejiang, China. ²The Key Laboratory for Quality Improvement of Agricultural Products of Zhejiang Province, College of Agricultural and Food Science, Zhejiang A&F University, Linan, Zhejiang, China. ³School of Mathematical & Natural Sciences, New College of Interdisciplinary Arts & Sciences, Arizona State University, Phoenix, AZ, USA. ⁴Zhejiang Dean Biotechnology Co. Hangzhou, Zhejiang, China. Correspondence and requests for materials should be addressed to D.Z. (email: zhangdayu@zafu.edu.cn)

Name	ORF	Amino acids	MW	Theoretical pI	Instability index	GRAVY
TmELO1	1005	334	39200.6	9.31	41.55	-0.041
TmELO2	972	323	38357.8	9.29	35.06	-0.021

Table 1. Sequence characters of TmELOs.

isolated and characterized in a handful of arthropod species including *Drosophila melanogaster* and *Aedes albopictus*²¹, the ELOs and ELOVLs in insects are poorly understood and require further investigation^{4,22,23}. The yellow mealworm beetle, *Tenebrio molitor*, is a species that has abundant fatty acids including VLCFAs, yet the *T. molitor* elongases associated with VLCFA synthesis have not been identified. In this study, we identified and characterized two elongases (*TmELO1* and *TmELO2*) of Very Long-Chain Fatty Acids of *T. molitor*. These two ELOs were chosen out of the 20 putative ELOs identified from a transcriptome analysis due to the availability of full length sequences. Functions of *TmELO1* and *TmELO2* were analyzed using both an *in vitro* expression system in yeast and *in vivo* RNA interference in mature *T. molitor* larvae.

Results

Sequence Analysis of ELOs from *T. molitor*. The open reading frames (ORFs) of full-length *TmELO1* (GenBank accession no. MF279188) and *TmELO2* (GenBank accession no. MF279189) were identified by DNASTar and the physical and chemical properties of the deduced proteins were calculated using the ProtParam tool of ExPASy²⁴ (Table 1). The instability index suggested that *TmELO2* was a relatively stable peptide of 323 aa, and *TmELO1* was of similar length at 334 aa but more unstable than *TmELO2*. The grand average of hydropathicity (GRAVY) shows that both *TmELO1* and *TmELO2* are hydrophilic. Further analysis indicates the presence of 5 putative transmembrane regions in *TmELO1* (27–46, 66–88, 171–193, 205–224, 234–251 amino acids) and 7 for *TmELO2* (25–47, 68–90, 116–135, 142–161, 171–193, 205–227, 237–254 amino acids). Prediction of subcellular locations using Euk-mPLoc 2.0^{25–27} suggests that both *TmELO1* and *TmELO2* were localized to the endoplasmic reticulum, the primary site of LCFA and VLCFA synthesis. Secondary structures of both *TmELO1* and *TmELO2* were predicted to be relatively similar to one another. Protein secondary structure prediction of *TmELO1* showed the percentage of α -helixes, β -turns, random coils, and extended strands among the total amino acids to be 34.7%, 6.9%, 29.3% and 29.0%, respectively. The percentage in *TmELO2* was 38.4% α -helixes, 8.1% β -turns, 23.2% random coils, and 30.3% extended strands.

Multi-sequencing alignment of the TmELOs with ELOs from other species showed that the proteins had some similar motifs such as KXXEXXDT, HXXMYXYY, TXXQXXQ and HXXHH, a histidine-box motif that is conserved in all elongases²⁸ (Fig. 1). The *TmELO1* and *TmELO2* had the highest identity at 92.51% with *Tribolium castaneum* LOC660197 and 88.62% with *T. castaneum* LOC660257 respectively, two uncharacterized predicted elongases. Compared with *D. melanogaster* elongases, *TmELO* had identity at 60.17% with CG31523, an uncharacterized, predicted elongase in *D. melanogaster* (Genbank accession no. NP_649474.1). The *TmELO* sequences shared 17.18–43.79% identity with *Homo sapiens* with HsELOVL7 being the most similar. The *TmELO* sequences had low identity to *S. cerevisiae* with the highest identity being only 18.67%.

A phylogenetic tree was constructed comparing the amino acid sequences of *T. molitor* elongases 1 and 2 with elongases from other organisms (Fig. 2). The phylogenetic analysis shows that *TmELO1* clustered with *T. castaneum* LOC660197 and *D. melanogaster* CG31523 while *TmELO2* clustered with *T. castaneum* LOC660257 and *D. melanogaster* CG2781, another predicted member of the ELO family.

Relative transcript level at developmental stages. Expression profiles of *TmELO1* and *TmELO2* at various developmental stages were generated using qRT-PCR (Fig. 3). Expression of both elongases was detected throughout all developmental stages examined. Expression of *TmELO1* peaked in 1st instar larvae and pupae while *TmELO2* peaked in embryos and was somewhat reduced throughout the remaining developmental stages. During embryonic development, expression of *TmELO2* was significantly higher than *TmELO1*. Expression of *TmELO1* was significantly higher than *TmELO2* throughout all other stages examined.

Fatty acid compositions and effects of RNAi. Total fatty acid compositions of mature larvae are listed in Table 2. The major fatty acids of *T. molitor* were C14:0, C16:0, C18:0, C18:1 and C18:2. Saturated fatty acids (SFAs), monounsaturated fatty acids (MUFAs) and polyunsaturated fatty acids (PUFAs) were 25.55%, 32.26% and 41.25%, respectively. The fatty acids (C > 16) were 81.2%.

Double-stranded RNA (dsRNA) fragments were generated for gene silencing using RNA interference. The dsRNA fragment lengths of *TmELO1* were 361 bp (dsELO1-1) and 298 bp (dsELO1-2), and *TmELO2* were 401 bp (dsELO2-1) and 342 bp (dsELO2-2), respectively. The relative transcript levels of *TmELO1* and *TmELO2* in dsRNAs-injected mature larvae decreased significantly at 1d, 2d, 3d and 4d after injection (Fig. 4). One day after injection, the transcript level of *TmELO1* was significantly reduced by 76.5–81.3% and *TmELO2* was significantly reduced by 75.8–86.7%. Both *TmELO* genes were largely suppressed after 1d, 2d, 3d and 4d, which showed that the dsRNA had a long-lasting effects on the *TmELO1* and *TmELO2* expression. Fatty acid compositions in the survivors after RNAi injections were not significantly different than controls (data not shown), however, dsRNA injection was associated with increased larval mortality (Fig. 4). Compared to the control, mortality after *TmELO1* RNAi treatment significantly increased to 50.8%, while, the mortality following *TmELO2* RNAi treatment was slightly, but not significantly higher than controls.

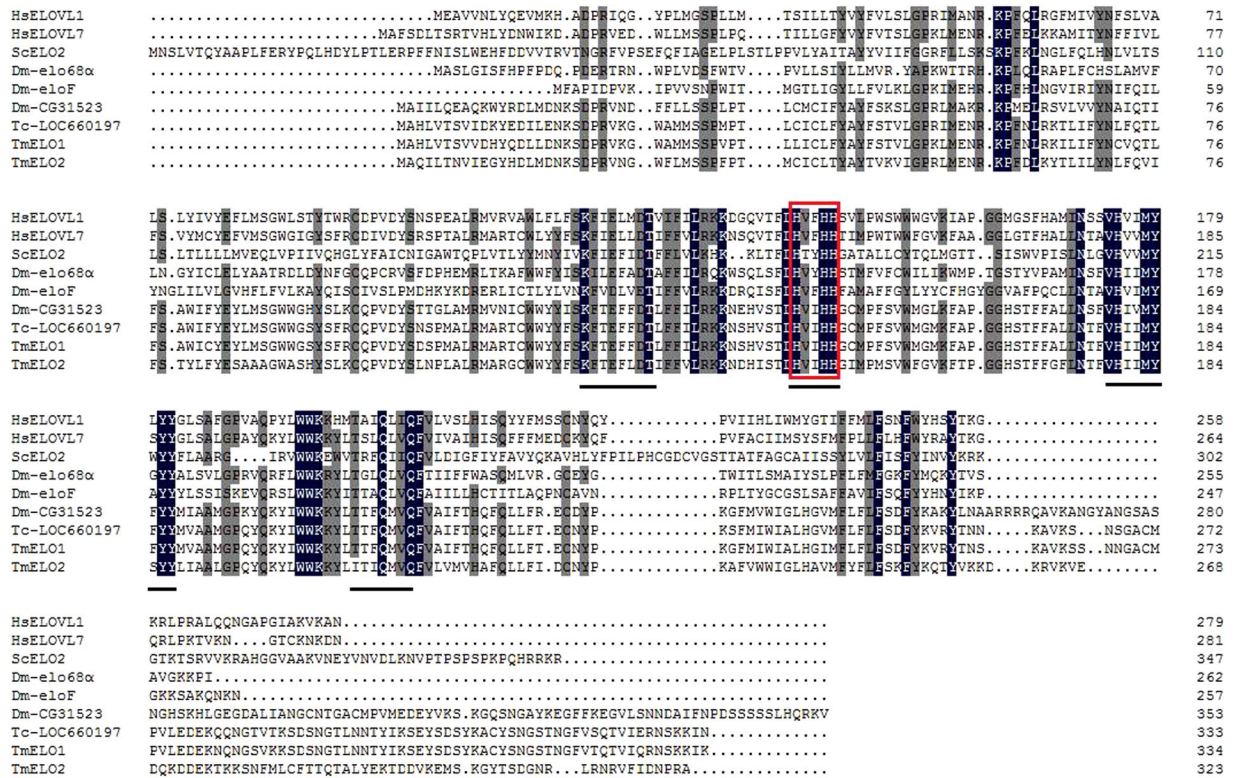


Figure 1. Multi-sequencing alignment of *TmELO1* and *TmELO2* with *H. sapiens* ELOVL1 and ELOVL7 (Genbank accession no. KJ894579.1 and AB181393.1), *S. cerevisiae* ELO2 (Genbank accession no. NM_001178748.1), *D. melanogaster* elo68 α (CG32072), eloF (CG16905), CG31523 (Genbank accession no. AJ871925.1, AM292552.1 and NP_649474.1), *T. castaneum* LOC660197 (Genbank accession no. XM_966451.3). The similar motifs which were marked by black lines are distinctive signs to the ELONGASE protein families. The conserved histidine motif HXXHH in the centre of the protein is boxed.

In-vitro functional characterization of TmELOs. The ORFs of *TmELO1* and *TmELO2* cDNA were isolated from *T. molitor*, cloned into a pYES2 yeast expression vector, and the recombinant plasmids were introduced into yeast strain INVSc1. Transcripts of two TmELOs were detected by RT-PCR in the TmELO-transformed yeast (Fig. 5). The fatty acid analysis of transformed yeast showed *TmELO1* expression increased relative amounts of C14:0, C16:0, C16:1 and C 20:0, and C24:0 fatty acids and reduced C18:0 fatty acids when compared with controls (Table 3). Expression of *TmELO2* in yeast increased relative amounts of C14:0, C14:1, C16:0, C16:1 fatty acids and reduced C18:1 fatty acids. In general, our observations suggest that in yeast, *TmELO1* could produce C20:0 and elongate SFA to C24; *TmELO2* primarily increases the percentage of C16:0 and C16:1. (Table 3).

Discussion

Tenebrio molitor larvae contain a large proportion of C \geq 16 fatty acids including LCFAs and VLCFAs and here we characterize two elongases, *TmELO1* and *TmELO2* that are involved in their synthesis. Both *TmELO1* and *TmELO2* are expressed throughout the lifetime of *T. molitor* and do not exhibit sex-specific expression. During embryonic stages, *TmELO2* appears to be the predominant form while *TmELO1* is expressed at higher levels throughout the remaining developmental stages. Our results are consistent with findings in mammals that demonstrate developmental regulation of different elongases, and that expression is regulated not only by developmental signals but also by diet²⁹. The effect of diet on *T. molitor* ELOVLs during development is intriguing but is outside the scope of the current study.

In the present study, expression of *T. molitor* elongases in yeast cells demonstrates differences in the fatty acids produced by *TmELO1* and *TmELO2* (Table 3). Expression of *TmELO2* led to significant increases of fatty acids up to 16 carbons in length, suggesting that *TmELO2* function is limited to long-chain fatty acid synthesis. Meanwhile, *TmELO1* expression led to similar increases in long-chain fatty acids but also produced a significant increase in C20 fatty acids and slight, but not significant increases in C22, and C24 fatty acids, suggesting that *TmELO1* may possess an additional role in the synthesis of very long-chain fatty acids. Surprisingly, RNAi-mediated knockdown of *TmELO1* and *TmELO2* in *T. molitor* did not significantly alter the fatty acid composition (data not shown). The lack of significant changes suggests that residual *TmELO1* and *TmELO2* transcript remained following RNAi treatment. It is also likely that *T. molitor* elongases have redundant roles and can maintain fatty acid levels in the absence of *TmELO1* or *TmELO2* activity. In support of the idea of redundant roles of elongases, ELOs in other species also have broad and somewhat overlapping functions. For example, in humans, HsELOVL1 can elongate C20–C26 SFAs³⁰, while HsELOVL3 can elongate FAs from C16 to C22².

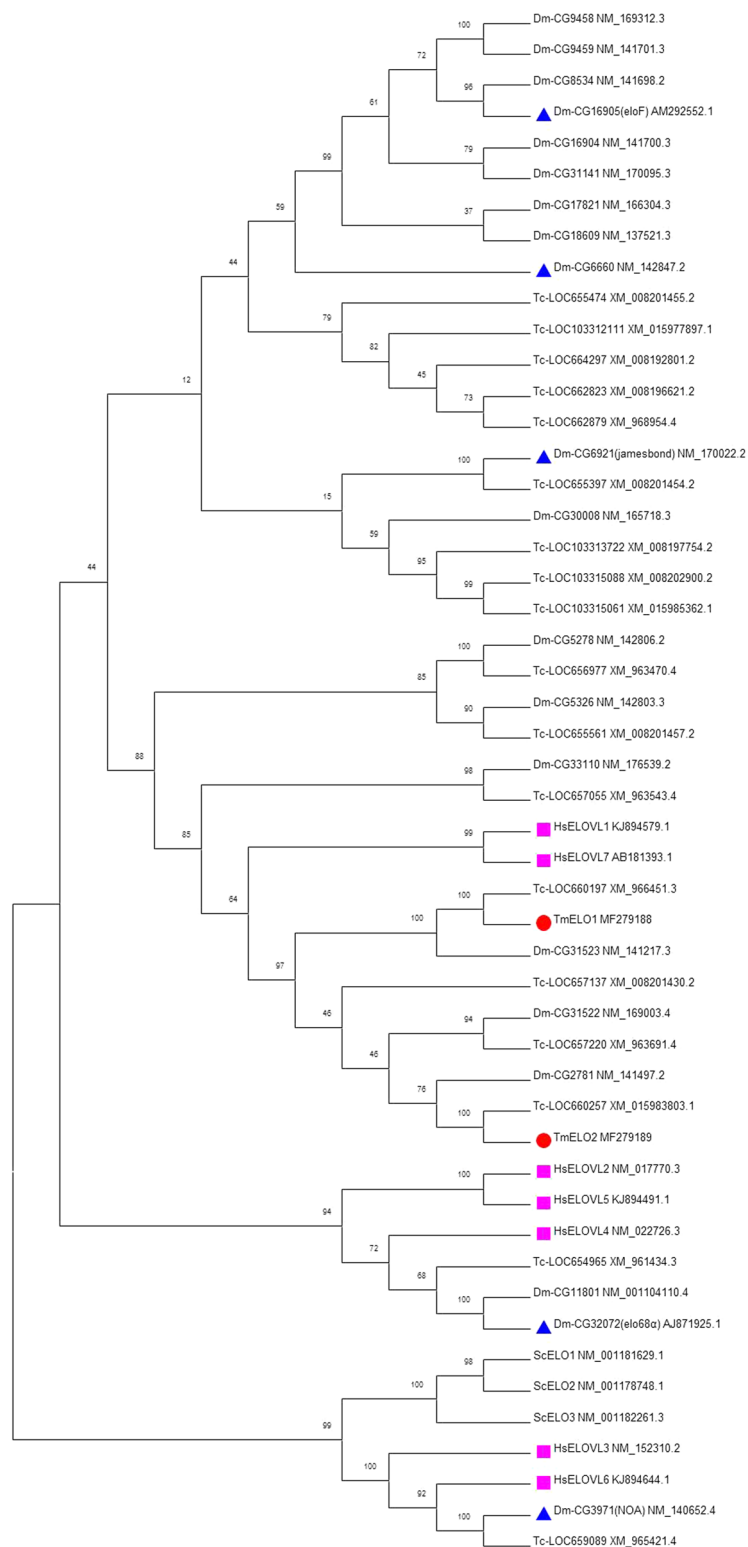


Figure 2. Phylogenetic tree of ELO included *H. sapiens* ELOV1-7 (marked by Purple squares), *S. cerevisiae* ELO1-3, all 20 *D. melanogaster* ELOs, 18 *T. castaneum* ELOs and TmELO1-2. Blue triangles indicate ELO which have been studied in insects. The phylogenetic tree was constructed using Neighbor-Joining method with 1000 bootstrap replicates. Each species was followed by its Genbank accession number.

Our observation that the two TmELOs generate FAs of different lengths is not unprecedented. In mammals, ELOV1-7 play different roles in the elongation cycle of fatty acids^{2, 31, 32}. ELOV1 produces C20 to C26 SFAs and MUFAs³⁰. ELOV2 can elongate C20 to C22 PUFAs³³. ELOV3 can elongate FAs from C16 to C22, with the

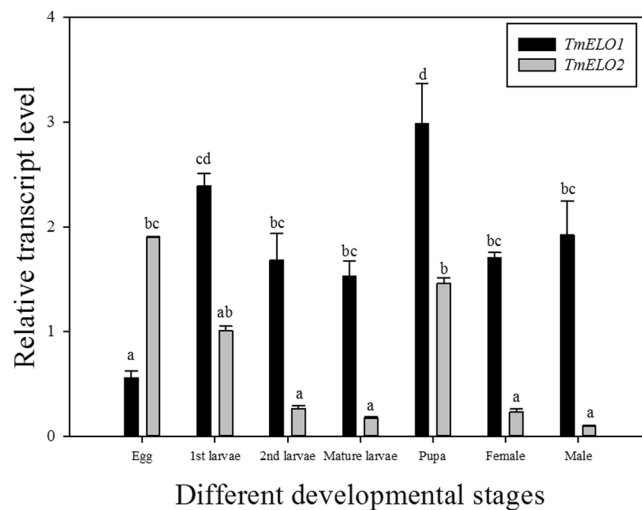


Figure 3. Relative transcript level of *TmELO1* and *TmELO2* at different developmental stages of *T. molitor*. The transcript levels of *TmELO1* and *TmELO2* at different developmental stages were conducted by qRT-PCR using RpS3 as a reference housekeeping gene. Y axis values are mean \pm SE of relative expression levels; Lowercase letters (a–d) represent significant differences ($P < 0.05$) according to Tukey's multiple range test.

Fatty acid	weight percent (n = 4)
C12:0	0.25 \pm 0.02
C14:0	2.17 \pm 0.04
C15:0	0.13 \pm 0.00
C16:0	15.63 \pm 0.19
C16:1	1.63 \pm 0.05
C17:0	0.29 \pm 0.01
C17:1	0.12 \pm 0.01
C18:0	5.97 \pm 0.16
C18:1	30.21 \pm 0.36
C18:2	40.53 \pm 0.34
C18:3	0.72 \pm 0.01
C20:0	0.37 \pm 0.01
C20:1	0.19 \pm 0.00
C20:2	0.61 \pm 0.11
C22:0	0.53 \pm 0.01
C22:1	0.11 \pm 0.02
C24:0	0.21 \pm 0.06
Total SFA	25.55
Total MUFA	32.26
Total PUFA	41.25

Table 2. Fatty acid compositions of mature *T. molitor* larvae. Note: The values are shown the percentage of total FAs as means \pm SE. n represents the number of independent samples.

highest activity toward C18-CoAs². ELOVL4 is specialized to elongate ultra long-chain fatty acids (ULCFAs) which are longer than C26^{34,35}. ELOVL5 elongates FAs from C18 to C20³⁶. ELOVL6 can elongate C12:0 FAs to C16:0³⁷. Finally, ELOVL7 has highest activity toward C18:3n-3 FA and C18:3n-6 FA^{38,39}.

Three ELOs of *S. cerevisiae* also showed variable functions. ScELO1 can elongate C14 FAs to C16 FAs¹² while ScELO2 is involved in the synthesis of SFAs and MUFAs to C24 and ScELO3 is essential for the synthesis of C24:0 to C26:0 and can also elongate a wide range of SFAs and MUFAs¹³. Similar results were also observed in *Drosophila*. Chertemps *et al.* (2005) reported an elongase gene named *elo68 α* in *Drosophila* males which can elongate myristoleic and palmitoleic acids (C14:1n-9 and C16:1n-9) *in-vitro* expression in yeast²². Chertemps *et al.* (2007) found that *eloF* cDNA of *D. melanogaster* expressed in yeast could elongate medium-chain saturated and unsaturated fatty acids up to C30⁴.

In *T. molitor*, silencing of *TmELO1* via RNAi resulted in an increased mortality rate indicating that *TmELO1* is essential for mealworm survival. Similar requirements for elongases in organism survival have been reported in other species. For example, in *Drosophila*, RNAi to CG6660, which encodes a predicted elongase, induced a

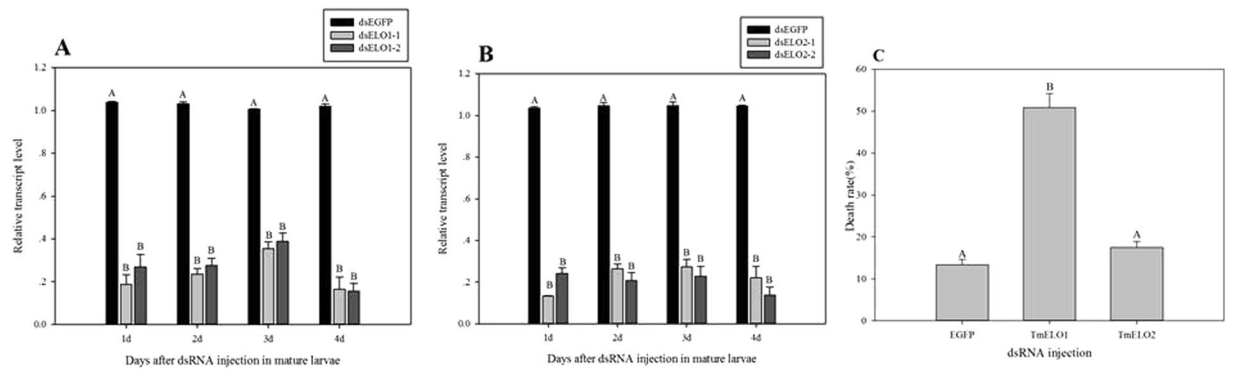


Figure 4. The dsRNA-mediated suppression of (A) *TmELO1* and (B) *TmELO2* transcripts in mature larvae. 5000 ng dsRNA was injected in every larva. Students t test was used in data analysis. Y axis values are mean \pm SE of relative transcript level. Uppercase letters (A–C) represent significant differences ($P < 0.01$) according to Tukey's multiple range test. (C). Mature larvae of *T. molitor* were injected with dsRNA of EGFP or *TmELO1* or *TmELO2*. There were three replicates and each replicate included 40 mature larvae. Y axis values are mean \pm SE of the death rate. Uppercase letters (A,B) represent significant differences ($P < 0.01$) according to Tukey's multiple range test.

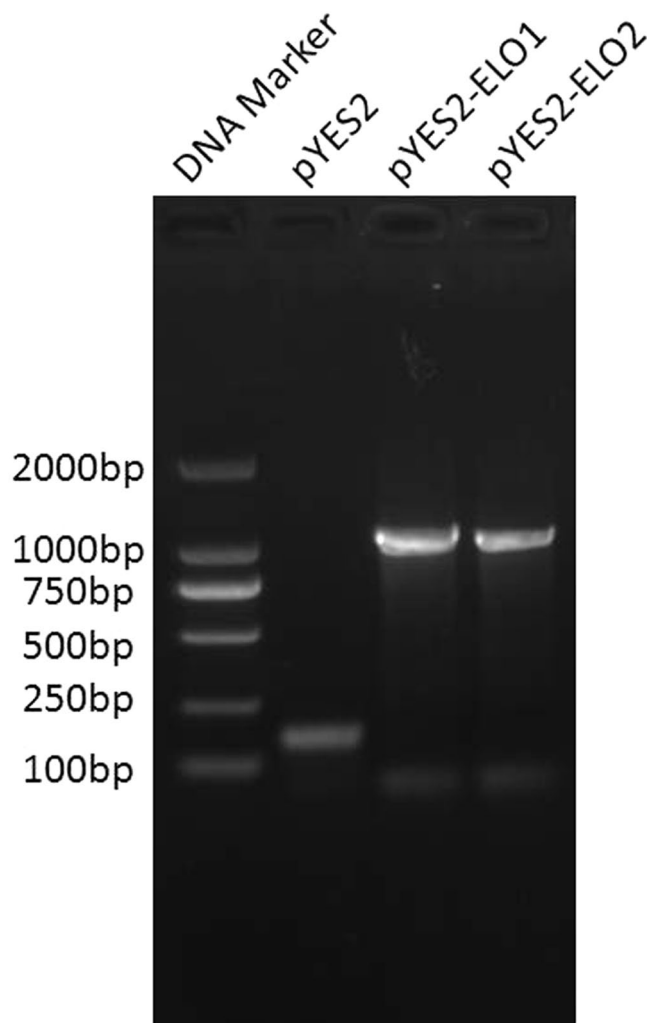


Figure 5. Reverse transcription (RT)-PCR analysis of *TmELO* transcripts in the transformed yeast lines. The RNA was isolated from the yeast that was transformed with recombinant plasmid and induced 24 h by galactose. PCR was conducted with CYC1 and T7 primers.

Fatty acid	Control(%)	TmELO1(%)	TmELO2(%)
C14:0	1.52 ± 0.04	2.12 ± 0.01*	2.03 ± 0.04*
C14:1	0.44 ± 0.00	0.79 ± 0.01*	0.55 ± 0.01*
C16:0	19.52 ± 0.15	20.04 ± 0.13	21.58 ± 0.33*
C16:1	41.65 ± 0.05	44.13 ± 0.19*	44.13 ± 0.23*
C18:0	8.28 ± 0.11	7.75 ± 0.17	9.46 ± 0.38
C18:1	28.38 ± 0.20	23.22 ± 0.16*	22.12 ± 0.43*
C20:0	n.d.	1.82 ± 0.03*	n.d.
C22:0	n.d.	Trace	n.d.
C24:0	n.d.	Trace	n.d.

Table 3. Fatty acid contents in yeast INVSc1 with or without expressed *TmELOs*. Results are means ± SE ($n = 4$). *Values for contents of fatty acids in yeast transformed with TmELO1 or TmELO2 are significantly different from control as determined by the Student t test ($P < 0.05$). Trace, FA was detected at low levels, but not in all samples.

similar lethal phenotype⁴⁰. Elongases have also been shown to be required for neonatal survival in mice⁴¹, survival of the protozoan parasite, *Toxoplasma gondii*⁴², and growth and survival of cancer cells⁴³. Together, these studies emphasize that the requirement for elongases in growth, development, and survival is likely conserved among metazoans.

Materials and Methods

Insects. *T. molitor* were obtained from Shandong Agricultural University and have been reared in our laboratory at Zhejiang A&F University for two years. The artificial climate chambers were maintained at $26 \pm 1^\circ\text{C}$, $65 \pm 5\%$ relative humidity and a 8:16 (L:D) photoperiod. The mealworm were reared on wheat bran mixed with cabbage.

Cloning of *TmELO* cDNAs. Total RNA was extracted from different stages of *T. molitor* using RNAiso Plus (TAKARA, Dalian, China), per the manufacturer's protocol and resulting RNA was stored at -80°C . The concentration and quality of total RNA was measured with a UV/VIS spectrophotometer (BioDrop μLite , Cambridge, UK) and agarose gel electrophoresis was used to verify integrity of the RNA. The 500ng total RNA was used in cDNA synthesis reactions using the PrimeScriptTM 1st strand cDNA Synthesis kit (TAKARA, Dalian, China) and resulting cDNA was stored at -20°C . *De novo* transcriptome sequencing was conducted at Tianke High-Tech Development Co., Ltd. (Zhengjiang, China) and the transcriptome analysis of *T. molitor* was performed in our laboratory (data not shown). The specific primers used to amplify two putative *ELO* genes are listed in Table 4. The PCR conditions for all these amplicons were 35 cycles of 94°C for 15 s, 55°C for 30 s and 72°C for 1 min. A 3'A-overhang was generated by *Taq* DNA polymerase (TAKARA), and amplified products were gel purified with an E.Z.N.A gel extraction kit (Omega bio-tek, Norcross, GA) and linked with a plasmid pMD19-T vector (TAKARA) to form a recombinant plasmid, which was then transformed into *DH5 α* (*E. coli*) for 10 hrs cultivation in LB solid medium with 50 $\mu\text{g}/\text{ml}$ ampicillin. The plasmids were sequenced with sequence-specific primer M13 and maintained as glycerol stocks at -80°C .

Sequence characterization of *TmELOs*. Full-length cDNA, *ELO* nucleotide sequences were translated into amino acid sequences and chemical and physical characteristics of *TmELO* genes were determined by the Expert Protein Analysis System program (<http://web.expasy.org/protparam/>)²⁴. Trans-membrane structures were calculated using the TMHMM Server v.2.0 (<http://www.cbs.dtu.dk/services/TMHMM/>). Subcellular locations were predicted by Euk-mPLoc 2.0 (<http://www.csbio.sjtu.edu.cn/bioinf/euk-multi-2/>)²⁵⁻²⁷. SOMPA⁴⁴ was used for the prediction of protein secondary structure. Amino acid sequences of other species *ELOs* were obtained from NCBI (<http://www.ncbi.nlm.nih.gov/>) and a phylogenetic tree was constructed and analyzed with respect to its homolog using the Neighbor Joining method. A bootstrap consensus tree of 1000 replicates was used to evaluate branch strength for analysis using MEGA 6.06.

Preparation of dsRNA and injection. The dsRNA fragments of two *ELO* genes which were used to silence the corresponding mRNA transcripts were synthesized using the *in vitro* Transcription T7 Kit (TAKARA)⁴⁵ and the specific primers used are listed in Table 4. Plasmid pMD19-T vectors linked with amplified *TmELO1* and *TmELO2* were the templates. The quality and length of the dsRNA fragments were measured by BioDrop μLite (BioDrop, Cambridge, England) and electrophoresis. The fragments were purified and diluted into a final concentration of 1 $\mu\text{g}/\mu\text{l}$. All dsRNAs were stored at -20°C . Each of the two *ELO* dsRNA were injected separately into mature larvae of *T. molitor* and EGFP dsRNA was used as the control. The larvae were collected 1d, 2d, 3d and 4d after injection, flash-frozen in liquid nitrogen and stored at -80°C . Animals were observed daily and the death rate was recorded through the pupal and adult stages till two weeks after injection. Every sample contained 20 larvae ($n = 3$) which were injected with 5 μg dsRNA fragments.

Quantitative real-time PCR. Total RNA extraction from *T. molitor* and cDNA synthesis was conducted using the same procedures as Cloning of *TmELO* cDNAs. The cDNA products were diluted to 5 ng/ μl . Primers (Table 4) for PCR and dsRNA synthesis were designed according to *TmELO1* and *TmELO2* sequences. The

Primer name	Primer sequence (5'-3')	Purpose	
<i>TmELO1</i> -F	CTGTGCGGAAAACGGAAGAG	cDNA cloning	
<i>TmELO1</i> -R	ATTTGCCCCCTGAGTTAC		
<i>TmELO2</i> -F	AGTGACTTGTGTTCTGTG		
<i>TmELO2</i> -R	AATTGCATTACGCCCGAGG		
<i>eTmELO1</i> -F	<u>CGGGATCC</u> ATGGCTCACCTAGTTACCAG	yeast expression	
<i>eTmELO1</i> -R	<u>CCCTCGAG</u> CTATTTGATCTTCTTTGAG		
<i>eTmELO2</i> -F	<u>CGGGATCC</u> ATGGCACAAATATTAAC		
<i>eTmELO2</i> -R	<u>CCCTCGAG</u> TTACGCCCGAGGTTGTCT		
ds <i>TmELO1</i> -F1	<u>GATCACTAATACGACTCACTATAGGG</u> GTGTCCAAACACTGTTTCAG	dsRNA fragments	
ds <i>TmELO1</i> -R1	<u>GATCACTAATACGACTCACTATAGGG</u> ATTGCCGCCACCATGTAA		
ds <i>TmELO2</i> -F1	<u>GATCACTAATACGACTCACTATAGGG</u> CACGACCTCATGGATAAC		
ds <i>TmELO2</i> -R1	<u>GATCACTAATACGACTCACTATAGGG</u> TGGAGGGTCCGAAATGTGG		
ds <i>TmELO1</i> -F2	<u>GATCACTAATACGACTCACTATAGGG</u> ATGGCTCACCTAGTTACCAG		
ds <i>TmELO1</i> -R2	<u>GATCACTAATACGACTCACTATAGGG</u> GTTGACACCTGAAGCTGT		
ds <i>TmELO2</i> -F2	<u>GATCACTAATACGACTCACTATAGGG</u> CTAGATACGATCTTCTTCG		
ds <i>TmELO2</i> -R2	<u>GATCACTAATACGACTCACTATAGGG</u> TAGACCTATCCACCAGAC		
dsEGFP-F	<u>GATCACTAATACGACTCACTATAGGG</u> ATGGTGAGCAAGGGCGAGGAGC		
dsEGFP-R	<u>GATCACTAATACGACTCACTATAGGG</u> ATCACTAATACGACTCACTATAGGG		
q <i>TmELO1</i> -F	TACTCATCAGTCCAGCTTCT		qRT-PCR
q <i>TmELO1</i> -R	CACCGTTATTACTACTCTTACA		
q <i>TmELO2</i> -F	CACGCCGTCATGTTCTACT		
q <i>TmELO2</i> -R	ACGCCCGAGGGTTGTCTAT		
q <i>TmRpS3</i> -F	GTGGTCGTTTCTGGCAAAC		
q <i>TmRpS3</i> -R	CAACTCTCTTGCCTCAACA		

Table 4. Sequences of primers used in DNA cloning, dsRNA synthesis and qRT-PCR. Xho I site (GGATCC), BamH I site (CTCGAG) and T7 promoter sequences (GATCACTAATACGACTCACTATAGGG) are underlined.

qRT-PCR reaction consisted of 20 µl including 10 µl SYBR® *Premix Ex Taq*TM (TAKARA), 1 µl each of 10 µM forward and reverse primer, 1 µl of diluted cDNA and dd H₂O. Ribosomal protein S3 (*TmRpS3*) (Genbank No.KJ868729.1) was selected as a housekeeping gene for normalization. Two-step qRT-PCR was conducted on Bio-Rad CFX96 (Bio-Rad, Hercules, California, USA) under the following conditions: 95 °C for 3 min, followed by 40 amplification cycles of 15 s at 95 °C and 30 s at 55 °C. Melting curves were used to verify the specificity of amplifications. Three biological replicates were carried out per treatment. Relative quantification analysis was then calculated using the $2^{-\Delta\Delta Ct}$ formula⁴⁶.

Heterologous expression of *TmELO* ORFs in yeast. The open reading frames (ORFs) of *TmELO1* and *TmELO2* were amplified by *eTmELO*-F and *eTmELO*-R primers. Primer F and Primer R separately contain a Xho I site and a BamH I site (Table 4). After PCR, the products were digested with Xho I and BamH I, ligated into the yeast expression vector pYES2 (Invitrogen), and used to transform *E. coli* DH5α. The *E. coli* were cultured and recombinant pYES2-*TmELO1*, and pYES2-*TmELO2* plasmids were extracted from DH5α using an Endo-free Plasmid Mini Kit I (OMEGA) according to manufacturer instructions. The pYES2, pYES2-*TmELO1*, and pYES2-*TmELO2* plasmids were introduced into INVSc1 (*Saccharomyces cerevisiae*) using the lithium acetate method⁴⁷. A single colony was selected from INVSc1 strains transformed with pYES2 (as control), pYES2-*TmELO1* or pYES2-*TmELO2* plasmids, introduced into 15 ml of SC-U medium containing 2% glucose, and maintained overnight, with shaking, at 30 °C. The overnight cultured yeast was resuspended in 50 ml of SC-U medium containing 2% galactose and grown to an optical density (OD600) reached 0.4. Cells were harvested after 24 h at 30 °C with shaking, washed twice by dd H₂O and stored at −80 °C until the FA were analyzed.

FAs analysis. *T. molitor* larvae were homogenized and trans-methylated in 1% H₂SO₄ in methanol (v:v) at 80 °C for 2 h to prepare mealworm fatty acid methyl ester (FAME)(n = 4). Total lipid was extracted from yeast cells by using acidified glass beads to break cell wall for 10 min, and using chloroform:methanol (2:1, v-v) and 1% H₂SO₄ in methanol (v:v) at 80 °C for 2 h to prepare yeast FAME (n = 4). Mealworms and yeast FAME were added to 2 mL 0.9% NaCl and extracted twice with 2 ml of hexane. Hexane was subsequently removed by nitrogen gas and the total FAME was resuspended in 300 ml of hexane. After mealworms or yeast were homogenized, 100 µg C17:0 was added as an internal control. FAME were then extracted and analyzed by GC. The samples were analyzed on an Agilent 6890 N Gas Chromatograph (GC) equipped with a DB-23 column (60 m × 0.25 mm) with 0.25 µm film thickness. The following temperature program was employed: 160 °C for 1 min, then 10 °C/min to 240 °C, with He as carrier gas. F.A.M.E. Mix, C4-C24 (Supelco®) was used as the external standard.

References

- Calder, P. C. Functional Roles of Fatty Acids and Their Effects on Human Health. *J. Parenter. Enteral Nutr.* **39**, 18S–32S (2015).
- Sassa, T. & Kihara, A. Metabolism of very long-chain fatty acids: genes and pathophysiology. *Biomol. Ther.* **22**, 83–92 (2014).
- Juárez, M. P. Fatty Acyl-CoA Elongation in *Blatella germanica* integumental microsomes. *Arch. Insect Biochem.* **56**, 170–178 (2004).
- Chertemps, T. *et al.* A female-biased expressed elongase involved in long-chain hydrocarbon biosynthesis and courtship behavior in *Drosophila melanogaster*. *Proc. Natl. Acad. Sci. USA* **104**, 4273–4278 (2007).
- Teerawanichpan, P., Robertson, A. J. & Qiu, X. A fatty acyl-CoA reductase highly expressed in the head of honey bee (*Apis mellifera*) involves biosynthesis of a wide range of aliphatic fatty alcohols. *Insect Biochem. Mole.* **40**, 641–649 (2010).
- Cuvillier, O. Sphingosine in apoptosis signaling. *Biochim. Biophys. Acta.* **1585**, 153–162 (2002).
- Hannun, Y. A. & Luberto, C. Ceramide in the eukaryotic stress response. *Trends Cell Biol.* **10**, 73–80 (2000).
- Hannun, Y. A. & Obeid, L. M. The Ceramide-centric universe of lipid-mediated cell regulation: stress encounters of the lipid kind. *J. Biol. Chem.* **277**, 25847–25850 (2002).
- Nakamura, M. T., Yudell, B. E. & Loor, J. J. Regulation of energy metabolism by long-chain fatty acids. *Prog. Lipid Res.* **53**, 124–144 (2014).
- Bannenberg, G. & Serhan, C. N. Specialized pro-resolving lipid mediators in the inflammatory response: an update. *Biochim. Biophys. Acta.* **1801**, 1260–1273 (2010).
- Nugteren, D. H. The enzymic chain elongation of fatty acids by rat-liver microsomes. *Biochim. Biophys. Acta.* **106**, 280–90 (1965).
- Toke, D. A. & Martin, C. E. Isolation and characterization of gene affecting fatty acid elongation in *Saccharomyces cerevisiae*. *J. Boil. Chem.* **271**, 18413–18422 (1996).
- Oh, C. S., Toke, D. A., Mandala, S. & Martin, C. E. *ELO2* and *ELO3*, Homologues of the *Saccharomyces cerevisiae* *ELO1* gene, function in fatty acid elongation and are required for sphingolipid formation. *J. Boil. Chem.* **272**, 17376–17384 (1997).
- Leonard, A. E., Pereira, S. L., Sprecher, H. & Huang, Y. S. Elongation of long-chain fatty acids. *Prog. Lipid Res.* **43**, 36–54 (2004).
- Stanley-Samuelson, D. W. & Dadd, R. H. Long-chain polyunsaturated fatty acids: Patterns of occurrence in insects. *Insect Biochem.* **13**, 549–558 (1983).
- Howard, R. W. & Stanley-Samuelson, D. W. Fatty acid composition of fat body and malpighian tubules of the tenebrionid beetle, *Zophobas atratus*: Significance in eicosanoid-mediated physiology. *Comp. Biochem. Phys. Part B: Biochem. Mole. Biol.* **115**, 429–437 (1996).
- Spike, B. P., Wright, R. J., Danielson, S. D. & Stanley-Samuelson, D. W. The fatty acid compositions of phospholipids and triacylglycerols from two chinch bug species *Blissus leucopterus leucopterus* and *B. iowensis* (Insecta: Hemiptera; Lygaeidae) are similar to the characteristic dipteran pattern. *Comp. Biochem. Phys. Part B: Biochem. Mole. Biol.* **99**, 799–802 (1991).
- Buckner, J. S. & Hagen, M. M. Triacylglycerol and phospholipid fatty acids of the silverleaf whitefly: Composition and biosynthesis. *Arch. Insect Biochem.* **53**, 66–79 (2003).
- Stanley-Samuelson, D. W., Loher, W. & Blomquist, G. J. Biosynthesis of polyunsaturated fatty acids by the Australian field cricket, *Teleogryllus commodus*. *Insect Biochem.* **16**, 387–393 (1986).
- Shiple, M. M., Dillwith, J. W., Bowman, A. S., Essenberg, R. C. & Sauer, J. R. Changes in lipids of the salivary glands of the lone star tick, *Amblyomma americanum*, during feeding. *J. Parasitol.* **79**, 834–842 (1993).
- Urbanski, J. M., Benoit, J. B., Michaud, M. R., Denlinger, D. L. & Armbruster, P. The molecular physiology of increased egg desiccation resistance during diapause in the invasive mosquito, *Aedes albopictus*. *Proc. Biol. Sci.* **277**, 2683–2692 (2010).
- Chertemps, T., Duportets, L., Labeur, C. & Wicker-Thomas, C. A new elongase selectively expressed in *Drosophila* male reproductive system. *Biochem. Biophys. Res. Co.* **333**, 1066–1072 (2005).
- Szafer-Glusman, E. *et al.* A Role for very-long-chain fatty acids in furrow ingression during cytokinesis in *Drosophila* Spermatocytes. *Curr. Biol.* **18**, 1426–1431 (2008).
- Gasteiger, E. *et al.* Protein Identification and Analysis Tools on the ExPASy Server. In *The Proteomics Protocols Handbook* (eds Walker, J. M.) 571–607 (Humana Press, 2005).
- Chou, K. C. & Shen, H. B. Euk-mPLOC: A fusion classifier for large-scale eukaryotic protein subcellular location prediction by incorporating multiple sites. *J. Proteome Res.* **6**, 1728–1734 (2007).
- Chou, K. C. & Shen, H. B. A new method for predicting the subcellular localization of eukaryotic proteins with both single and multiple sites: Euk-mPLOC 2.0. *PLOS One* **5**, e9931 (2010).
- Chou, K. C. & Shen, H. B. Cell-PLOC: a package of Web servers for predicting subcellular localization of proteins in various organisms. *Nat. Protoc.* **3**, 153–162 (2008).
- Moon, Y. A., Shah, N. A., Mohapatra, S., Warrington, J. A. & Horton, J. D. Identification of a mammalian long chain fatty acyl elongase regulated by sterol regulatory element-binding proteins. *J. Biol. Chem.* **276**, 45358–45366 (2001).
- Wang, Y. *et al.* Tissue-specific, nutritional, and developmental regulation of rat fatty acid elongases. *J. Lipid Res.* **46**, 706–715 (2005).
- Ohno, Y. *et al.* ELOVL1 production of C24 acyl-CoAs is linked to C24 sphingolipid synthesis. *Proc. Natl. Acad. Sci. USA* **107**, 18439–18444 (2010).
- Jakobsson, A., Westerberg, R. & Jacobsson, A. Fatty acid elongases in mammals: Their regulation and roles in metabolism. *Prog. Lipid Res.* **45**, 237–249 (2006).
- Guilou, H., Zdravec, D., Martin, P. G. & Jacobsson, A. The key roles of elongases and desaturases in mammalian fatty acid metabolism: Insights from transgenic mice. *Prog. Lipid Res.* **49**, 186–199 (2010).
- Zdravec, D. *et al.* ELOVL2 controls the level of n-6 28:5 and 30:5 fatty acids in testis, a prerequisite for male fertility and sperm maturation in mice. *Chem. Phys. Lipids* **52**, 245–255 (2011).
- Li, W. *et al.* Depletion of ceramides with very long chain fatty acids causes defective skin permeability barrier function, and neonatal lethality in ELOVL4 deficient mice. *Int. J. Biol. Sci.* **3**, 120–128 (2007).
- Vasireddy, V. *et al.* Elov14 5-bp-deletion knock-in mice develop progressive photoreceptor degeneration. *Invest. Ophthalmol. Vis. Sci.* **47**, 4558–4568 (2006).
- Moon, Y. A., Hammer, R. E. & Horton, J. D. Deletion of ELOVL5 leads to fatty liver through activation of SREBP-1c in mice. *J. Lipid Res.* **50**, 412–423 (2009).
- Matsuzaka, T. *et al.* Crucial role of a long-chain fatty acid elongase, ELOVL6, in obesity-induced insulin resistance. *Nat. Med.* **13**, 1193–1202 (2007).
- Naganuma, T., Sato, Y., Sassa, T., Ohno, Y. & Kihara, A. Biochemical characterization of the very long-chain fatty acid elongase ELOVL7. *FEBS Lett.* **585**, 3337–3341 (2011).
- Purdy, J. G., Shenk, T. & Rabinowitz, J. D. Fatty acid elongase 7 catalyzes lipidome remodeling essential for human cytomegalovirus replication. *Cell Rep.* **10**, 1375–1385 (2015).
- Parvy, J. P. *et al.* *Drosophila melanogaster* Acetyl-CoA-Carboxylase sustains a fatty acid-dependent remote signal to waterproof the respiratory system. *PLOS Genet.* **8**, e1002925 (2012).
- Cameron, D. J. *et al.* Essential role of Elov14 in very long chain fatty acid synthesis, skin permeability barrier function, and neonatal survival. *Int. J. Biol. Sci.* **3**, 111–119 (2007).
- Mazumdar, J., H Wilson, E., Masek, K., A Hunter, C. & Striepen, B. Apicoplast fatty acid synthesis is essential for organelle biogenesis and parasite survival in *Toxoplasma gondii*. *Proc. Natl. Acad. Sci. USA* **103**, 13192–13197 (2006).
- Röhrig, F. & Schulze, A. The multifaceted roles of fatty acid synthesis in cancer. *Nat. Rev. Cancer* **16**, 732–749 (2016).

44. Geourjon, C. & Deléage, G. SOPMA: significant improvements in protein secondary structure prediction by consensus prediction from multiple alignments. *Comput Appl Biosci*. **11**, 681–684 (1995).
45. Davanloo, P., Rosenberg, A. H., Dunn, J. J. & Studier, F. W. Cloning and expression of the gene for bacteriophage T7 RNA polymerase. *Proc. Natl. Acad. Sci. USA* **81**, 2035–2039 (1984).
46. Livak, K. J. & Schmittgen, T. D. Analysis of relative gene expression data using real-time quantitative PCR and the $2^{-\Delta\Delta CT}$ method. *Methods* **25**, 402–408 (2001).
47. Gietz, R. D., Schiestl, R. H., Willems, A. R. & Woods, R. A. Studies on the transformation of intact yeast cells by the LiAc/SS-DNA/PEG procedure. *Yeast* **11**, 355–360 (1995).

Acknowledgements

The authors would like to thank for the financial support from DEAN-ZAFU cooperative project (2045200233) and Developmental Fund of Zhejiang A&F University (2012FR087).

Author Contributions

T.X.Z., M.Z.W. and D.Y.Z. conceived and designed the experiments; T.X.Z. and H.S.L. performed the experiments; T.X.Z., N.H., S.Y. W. J.H.P. and D.Y.Z. analyzed the data; T.X.Z. J.H.P. and D.Y.Z. wrote the paper. All authors read and approved the final manuscript.

Additional Information

Competing Interests: The authors declare that they have no competing interests.

Publisher's note: Springer Nature remains neutral with regard to jurisdictional claims in published maps and institutional affiliations.



Open Access This article is licensed under a Creative Commons Attribution 4.0 International License, which permits use, sharing, adaptation, distribution and reproduction in any medium or format, as long as you give appropriate credit to the original author(s) and the source, provide a link to the Creative Commons license, and indicate if changes were made. The images or other third party material in this article are included in the article's Creative Commons license, unless indicated otherwise in a credit line to the material. If material is not included in the article's Creative Commons license and your intended use is not permitted by statutory regulation or exceeds the permitted use, you will need to obtain permission directly from the copyright holder. To view a copy of this license, visit <http://creativecommons.org/licenses/by/4.0/>.

© The Author(s) 2017